Progress In Electromagnetics Research Letters, Vol. 70, 23–30, 2017

Archimedean Spiral Antenna with Two Opposite Uni-Directional Circularly Polarized Radiation Bands Designed by Resonance Based Reflectors

Ji-Yang Xie[1], Lin Peng[1, 2, *], Bao-Jian Wen[1], and Xing Jiang[1]

Abstract—Two opposite uni-directional radiation bands with good circular polarization (CP) characteristics are achieved in an Archimedean Spiral Antenna (ASA). A sandwich configuration is formed by utilizing two resonance based reflectors (RBRs) at the bottom and top sides of the ASA. Owing to the resonance characteristic, the RBRs do not act as reflectors at the other operational band, then, opposite uni-directional radiations are obtained, and the two uni-directional bands can be tuned independently. The proposed ASA with two uni-directional bands (ASA-TUB) has a wide impedance bandwidth about 4.4 : 1 (1.8–8 GHz), while its front-fire band (FFB) ranges from 1.8 GHz to 2.2 GHz (20.0%), and its back-fire band (BFB) is 4.4–7.1 GHz (46.9%) for front-to-back ratio (FBR) larger than 5 dB. The maximal FBRs for the FFB and BFB are 11.3 dB and 20 dB, respectively. Moreover, good CP performances are also obtained for the FFB and BFB. Besides, the whole profile of the proposed antenna is only 0.16λ at the lowest operational frequency. The proposed antenna has the properties of dual opposite uni-directional radiation bands, low profile, good FBR and CP.

1. INTRODUCTION

Since the Archimedean spiral antenna (ASA) was first invented by J. A. Kaiser in 1960 [1], it have been well studied for very wideband, bi-directional radiation and circular polarization. However, some modern wireless systems require antennas with broadband, circular polarization, uni-direction and low-profile characteristics.

There are many methods to transform the bi-directional radiation of an ASA to be uni-directional radiation, such as backing the antenna by a cavity [2–4], using high impedance surface (HIS) and electromagnetic band-gap (EBG) as reflector [5–7] or loading a PEC reflector behind the antenna [8, 9].

However, it is bulky due to the cavity reflector [2], and the absorbing material (ABS) needs to be filled in the cavity to absorb backward electromagnetic waves, which may cause high loss in antenna applications [3, 4]. In [3], an ASA has an impedance bandwidth of 3–9 GHz with a 0.07λ profile by utilizing a cavity loaded ribbon ABS. However, the total efficiency of the antenna is less than 80% due to the ABS. An EBG structure can be used to obtain good uni-directional radiation. However, it may cause narrow impedance bandwidth [5], poor CP characteristics [6] and large gain variation [7]. In [8], the effects of a PEC on the performance of ASA were carefully studied, and it is found that there must be distance $\lambda/4$ from the ASA with PEC used as reflector for the antenna. To solve these problems, a novel reflector denoted as resonance based reflector (RBR) was proposed in [10], and it could be utilized to design uni-directional antenna.

Received 20 June 2017, Accepted 10 August 2017, Scheduled 24 August 2017

* Corresponding author: Lin Peng (penglin528@hotmail.com).

[1] Guangxi Key Laboratory of Wireless Wideband Communication and Signal Processing, Guilin University of Electronic Technology, Guilin, Guangxi 541004, China. [2] Guangxi Experiment Center of Information Science, Guilin University of Electronic Technology, Guilin, Guangxi 541004, China.

In this paper, two RBRs operated at different bands are used at the bottom and top sides of an ASA, respectively, to form a sandwich configuration. Thanks to the resonance characteristics of the RBRs, they do not behave as reflector for the other. Then, two opposite uni-directional pattern bands are obtained. The larger RBR at the bottom of the ASA realizes FFB from 1.8 GHz to 2.2 GHz with FBR larger than 5 dB, and the smaller RBR at the top of the ASA obtains BFB from 4.4 to 7.1 GHz. Meanwhile, good CP performances are also obtained for the FFB and BFB.

2. ANTENNA DESIGN AND RESULTS

2.1. Reference Archimedean Spiral Antenna

A referenced two-arm archimedean spiral antenna (RASA) is designed to work in the 1.5–8 GHz frequency range. The simulations in this research are conducted by CST MWS software [11]. A loading ring surrounds the RASA to miniaturize the size and improve the radiation patterns [12, 13]. The geometry and dimensions of the RASA are depicted in Fig. 1(a). The gap between the two adjacent arms is equal to the width of the arm, so the structure is a self-complementary structure. Note that because the ring surrounds the ASA as shown in Fig. 1(a), the input impedance of RASA is about 100 Ω. Meanwhile, a wide-band balun is used in order to transform the 100 Ω input impedance of the RASA to 50 Ω of a SMA connector, which is not presented in this letter for simplicity. For the RASA, the size of the substrate is $2 \times r$, while D and a_r are the outer and inner diameters of the RASA; a_w is the width of the arm, a_g the gap between the two adjacent arms and w_l the width of the loading ring. Four holes with diameter m are bored for the assembling of the RBRs. All parts of the design are printed on a substrate F4B-M with $\varepsilon_r = 2.65$ and thickness of 1 mm, and all values of the parameters shown in Fig. 1(a) are listed in Table 1.

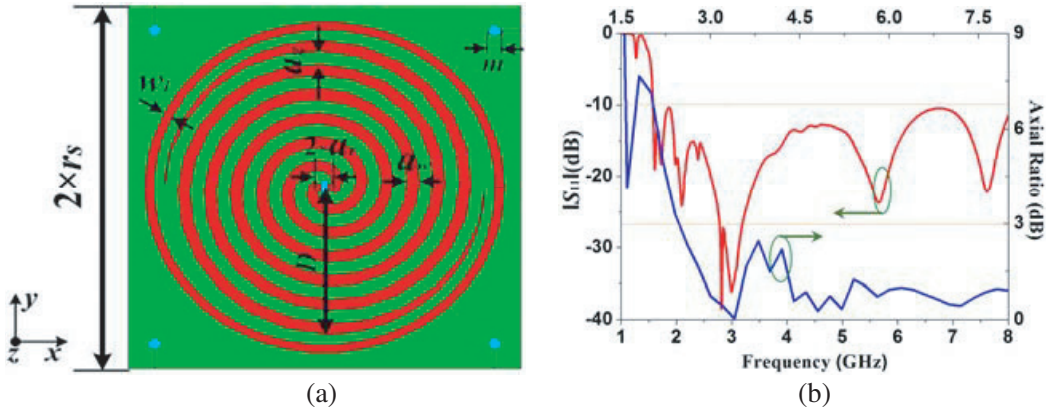

(a) (b)

Figure 1. The proposed RASA. (a) Top view. (b) Simulated $|S_{11}|$ and AR.

Table 1. Parameters of the RASA (mm).

Para.	D	a_r	a_w	a_g	w_l	r	m
Value	24.5	0.5	2	2	1	30	2

The simulated $|S_{11}|$ and axial ratio curves of the RASA are plotted in Fig. 1(b). It is clearly shown that the impedance bandwidth of the ASA is about 5.3 : 1 (1.5 GHz–8 GHz), and good axial ratio (AR < 3 dB) is obtained in a wide bandwidth of 3.64 : 1 (2.2–8 GHz). Therefore, the RASA has good performances as a basis of the design.

2.2. The ASA with Two Uni-Directional Bands (ASA-TUB)

Though the RASA has excellent performances, its radiation pattern is bi-directional. To obtained two uni-directional pattern bands with opposite directions while maintaining wide-band and low-profile characteristics, two RBRs, called RBR 1 and RBR 2, are used as reflectors to the RASA. Note that when the reflectors are applied to the RASA, there is no returning work required for the previously determined dimensions.

The geometry and dimensions of RBR 1 and RBR 2 are shown in Fig. 2(a). The method to acquire the phase and amplitude of the reflection coefficient is presented in [10], thus, simulations are carried to obtain the characteristics of RBR 1 and RBR 2. It is supposed that an RBR is placed at a certain distance to the antenna to realize in-phase reflection ($-90° < \varphi < 90°$). Then, as shown in Fig. 2(a), reference planes are set to monitor the RBRs characteristics. h_{a1} is the distance between RBR 1 (port 2) and the reference plane (port 1), while h_{a2} is the distance between RBR 2 (port 3) and the reference plane (port 1). Parameters r_{g1} and r_{w1} are the radius and width of RBR 1, respectively. h_{a2} and r_{w2} are the radius and width of RBR 2, respectively. With the help of CST MWS software, all the optimal parameters are listed in Table 2.

The reflection phases of RBR 1 (φ_1) and RBR 2 (φ_2) are depicted in Figs. 2(b) and (c), respectively.

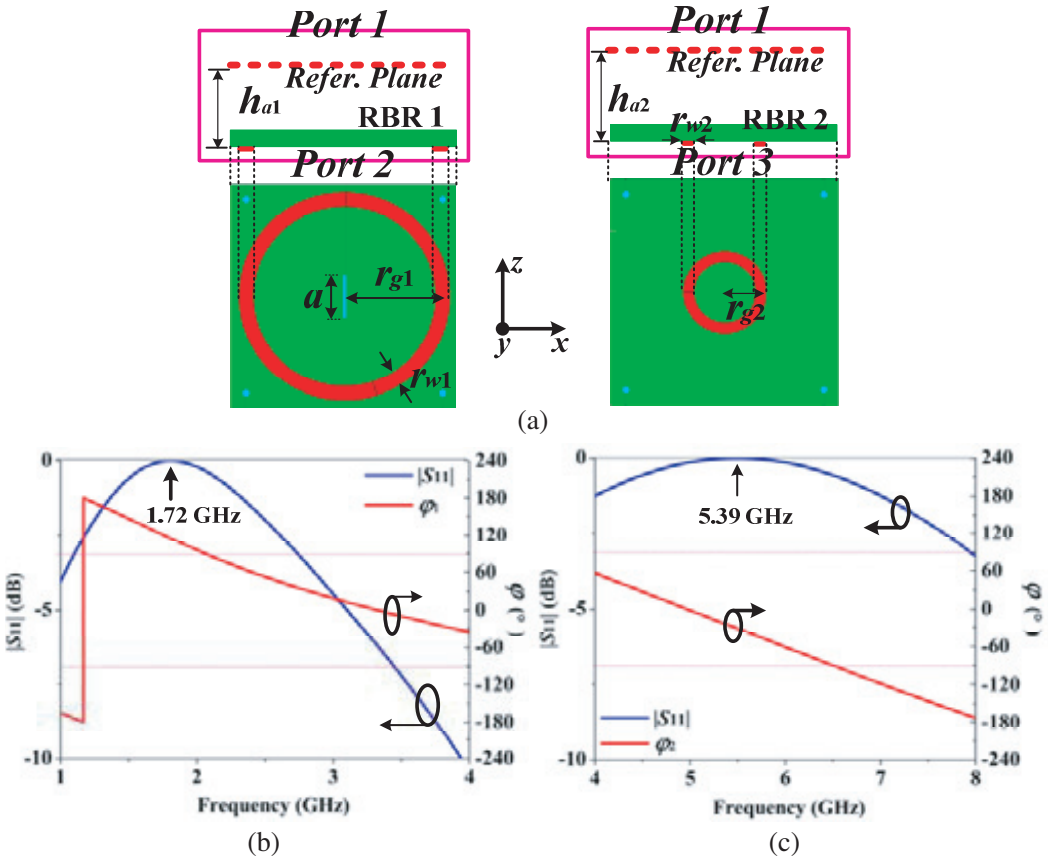

Figure 2. The RBRs. (a) Simulation diagrams and the dimensions of RBR 1 and RBR 2. (b) Characteristics of RBR 1. (c) Characteristics of RBR 2.

Table 2. Parameters of the ASA-TUB (mm).

Para.	$\mathbf{r}_{g1}$	$\mathbf{r}_{w1}$	$\mathbf{r}_{g2}$	$\mathbf{r}_{w2}$	$\mathbf{h}_{a1}$	$\mathbf{h}_{a2}$
Value	28	4	11	3	10	16

Note that φ_1 and φ_2 are the reflection phases at the reference planes. $|S_{11}|$ (reflection coefficient) curves are also plotted in the figures. The in-phase reflection bands ($-90° < \varphi < 90°$) of RBR 1 and RBR 2 are 2–4 GHz and 4–6.6 GHz, respectively. As marked in Figs. 2(b) and (c), the resonant frequencies of RBR 1 and RBR 2 are 1.72 GHz and 5.39 GHz, respectively.

After obtaining the reflection characteristics of RBR 1 and RBR 2, the ASA-TUB can be designed. The RBRs are applied to the RASA to form an ASA-TUB as shown in Fig. 3(a), while Fig. 3(b) shows the simulated and measured $|S_{11}|$ of the ASA-TUB. Obviously, there is a wide impedance bandwidth

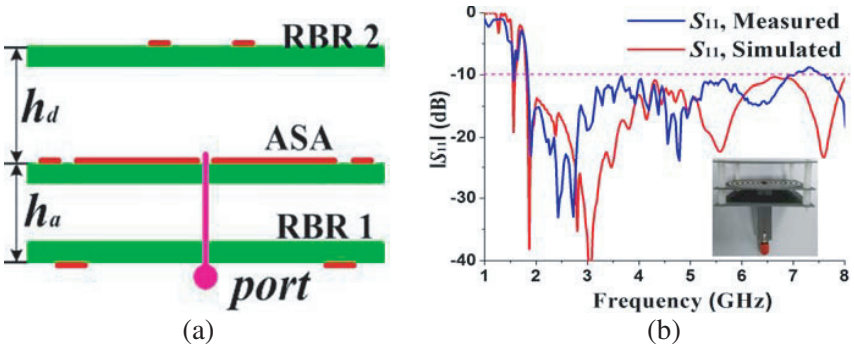

Figure 3. ASA-TUB. (a) Side view. (b) The simulated and measured $|S_{11}|$.

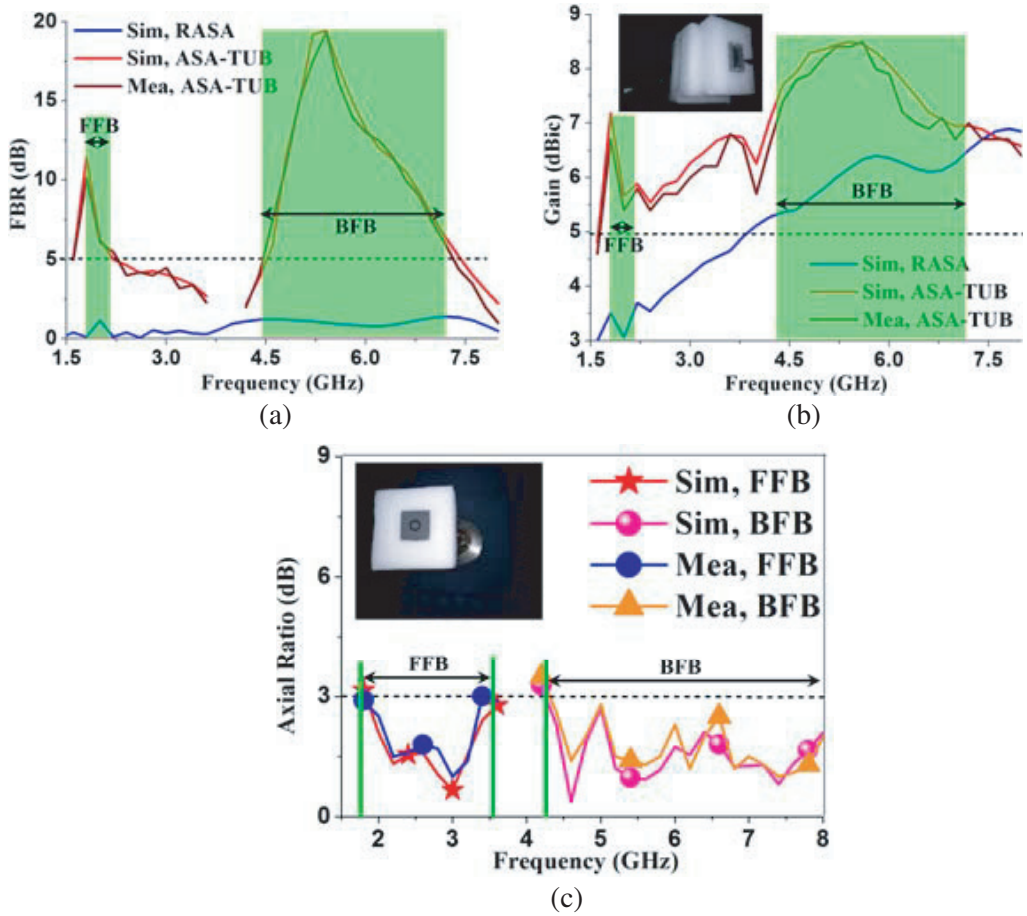

Figure 4. Results. (a) The comparison of FBR. (b) The comparison of gain. (c) The simulated and measured AR.

for ASA-TUB of 1.8–8 GHz. Good agreement is obtained between simulated and measured results. The simulated and measured FBRs and gain curves of the RASA and ASA-TUB are depicted in Figs. 4(a) and (b) for comparison. It is obvious that two uni-directional bands are obtained. Good agreements are observed between simulations and measurements. And, the FBR is enhanced from about 0 dB to 11.3 dB at 1.8 GHz and 20 dB at 5.3 GHz. Note that the maximum FBR is very close to the resonant frequencies of the two RBRs. Furthermore, it is found from Fig. 4 (b) that the peak gains of the FFB and BFB are about 7.3 dBic and 8.5 dBic, respectively. And the gains of the FFB and BFB are 1.5–2 dB larger than their neighbors. Fig. 4(c) shows the simulated and measured AR curves of ASA-TUB, and the measured AR level of the ASA-TUB is less than 3 dB from 1.8 GHz to 3.6 GHz and 4.2 GHz to 8 GHz.

Finally, in order to further verify the opposite uni-directional bands of the ASA-TUB, the radiation patterns in *xoz* plane are measured. The radiation patterns at 1.8 GHz, 4.5 GHz and 5.4 GHz are plotted in Fig. 5. It is obvious that the ASA-TUB does radiate to the two opposite directions for FFB and

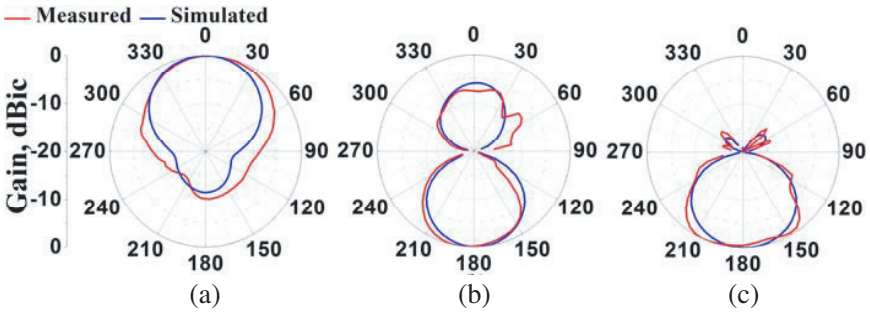

Figure 5. Radiation pattern of ASA-TUB for BFB. (a) 1.8 GHz. (b) 4.5 GHz. (c) 5.4 GHz.

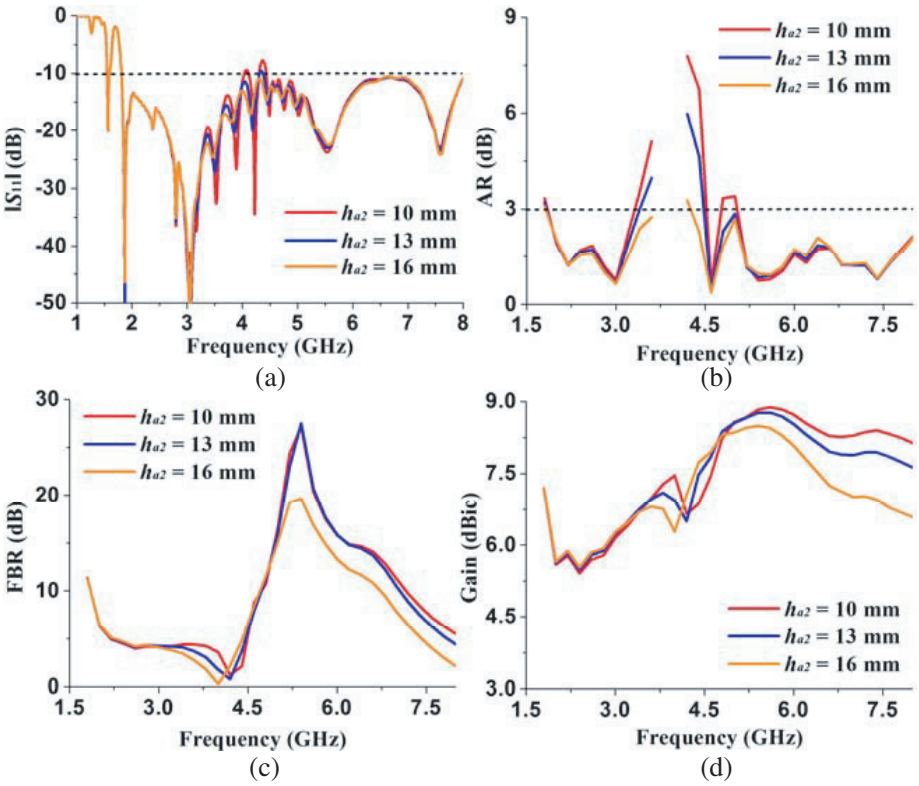

Figure 6. The performances of ASA-TUB while h_{a2} increases. (a) $|S_{11}|$. (b) AR. (c) FBR. (d) Gain.

BFB. As shown in Fig. 5(a), the FFB radiates to $+z$ direction, and the BFB radiates to $-z$ direction from Figs. 5(b) and (c). The measured results show good agreement with simulated ones.

2.3. Discussion

In order to further study the factors that affect the performances of the antenna, the parameters of RBR 2 are carefully discussed in this section. Note that all the studies are based on the ASA-TUB.

Firstly, h_{a2} is changed from 10 mm to 16 mm with a step of 3 mm when the r_{w2} and r_{g2} remain as 3 mm and 11 mm. The results are shown in Fig. 6. Fig. 6(a) shows the $|S_{11}|$ curves. It is obvious that parameter h_{a2} has little impact on the $|S_{11}|$ of ASA-TUB. Fig. 6(b) shows the AR of FFB and BFB. It can be found that the AR bandwidths of both FFB and BFB are reduced when h_{a2} is increased, and the AR of ASA-TUB is less than 3 dB in whole operational band when $h_{a2} = 16$ mm. The cause is that the coupling between RBR 2 and ASA-TUB affects the AR. Fig. 6(c) shows the FBR curves as the h_{a2} is increased. It is clear that the FBR in FFB is almost unchanged, while the FBR in BFB is increased. From Fig. 6(d), the antenna gain increases with decreased h_{a2}.

r_{w2} is scanned as 2 mm, 3 mm and 4 mm when h_{a2} and r_{g2} remain as 16 mm and 11 mm, respectively, with the results plotted in Fig. 7. When r_{w2} is increased, the $|S_{11}|$ in Fig. 7(a) is almost unchanged. Fig. 7(b) shows the AR of ASA-TUB in FFB and BFB, which presents good AR. As shown in Fig. 7(c), the FBR of FFB is almost unchanged, while the peak value of the FBR of BFB is shifted to higher frequency as r_{w2} is increased. This is because r_{w2} controls the resonance of RBR 2 and then the in-phase band. In addition, it can be obtained from Fig. 7(c) and Fig. 7(d) that the FBRs at high frequencies ($f > 4.5$ GHz) will increase with increasing r_{w2}, so the gains will also increase with increasing r_{w2} at high frequencies ($f > 4.5$ GHz). Thus, r_{w2} can be used to tune the operational frequencies of the BFB.

RBR 2 parameter r_{g2} is studied as 9 mm, 11 mm and 13 mm when r_{w2} and h_{a2} remain as 3 mm and 16 mm with the results shown in Fig. 8. As shown in Fig. 8(a), the $|S_{11}|$ presents some deterioration in 3–5 GHz as r_{g2} is increased. The deteriorated bands are related to the resonant frequency of RBR

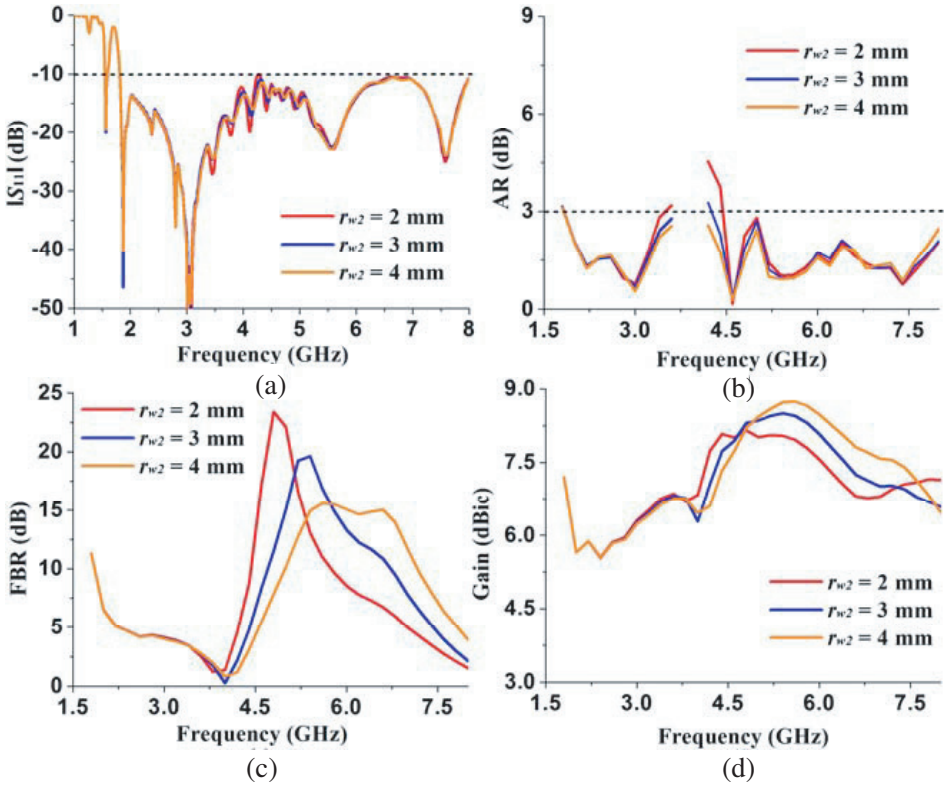

Figure 7. The performances of ASA-TUB while r_{w2} increases. (a) $|S_{11}|$. (b) AR. (c) FBR. (d) Gain.

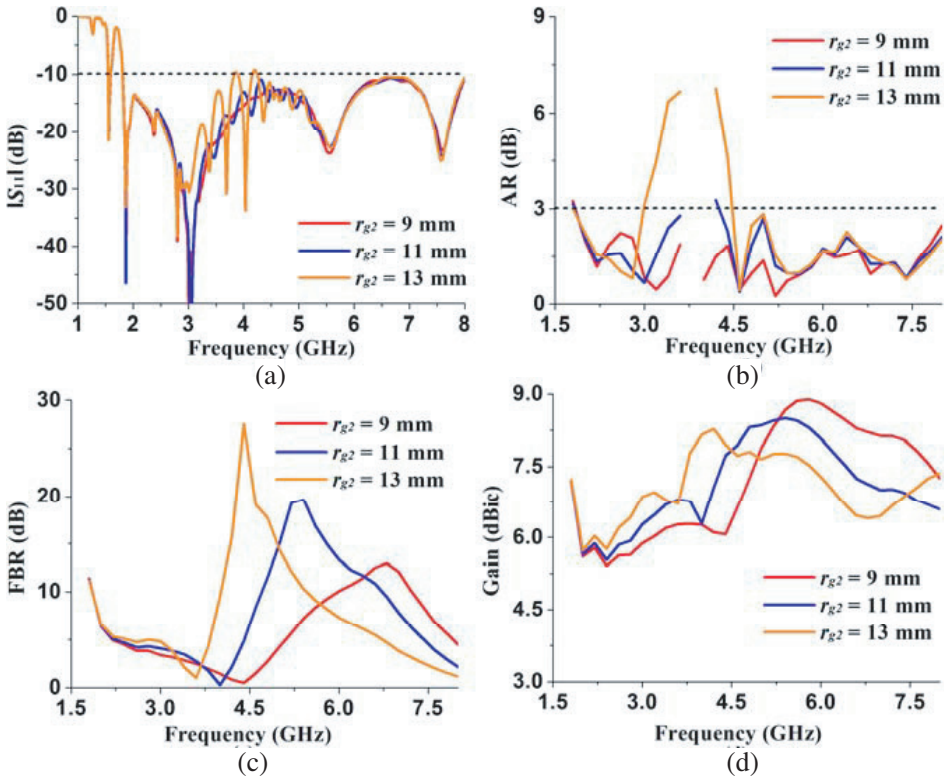

Figure 8. The performances of ASA-TUB while r_{g2} increases. (a) $|S_{11}|$. (b) AR. (c) FBR. (d) Gain.

2. It can be seen in Fig. 8(b) that the AR of ASA-TUB in FFB and BFB will somewhat deteriorate when r_{g2} increases. Fig. 8(c) shows the FBR of the antenna, while Fig. 8(d) shows the gain. It can be clearly seen that when r_{g2} is increased, the FBR in FFB is gradually increased, while in BFB the peak of FBR is shifted to lower frequency. Thus, r_{g2} can also be used to tune the operational frequencies of the BFB.

In summary, the parameters of RBR 1 and RBR 2 can be used to adjust the operational frequencies and AR characteristic of the FFB and BFB, respectively.

3. CONCLUSION

In this paper, a low-profile ASA with two opposite uni-directional CP bands (ASA-TUB) is designed. The two opposite uni-directional bands are achieved by loading two RBRs at the bottom and top sides of the RASA. The proposed ASA-TUB has a wide impedance bandwidth about 4.4 : 1 (1.8–8 GHz), and the front-fire band (FFB, 20.0%, 1.8–2.2 GHz) and back-fire band (BFB, 46.9%, 4.4–7.1 GHz). Good CP characteristics are also obtained. Meanwhile, the ASA-TUB is only 0.16λ at the lowest operational frequency. As the RBRs do not act as reflector for each other, the FFB and BFB are achieved, and the opposite uni-directional CP bands can be tuned easily.

ACKNOWLEDGMENT

This work was supported in part by the National Natural Science Foundation of China under Grant Nos. 61661011 & 61401110 & 61371056, in part by Natural Science Foundation of Guangxi under Grant No. 2015GXNSFBA139244, and in part by Innovation Project of GUET Graduate Education under Grant No. 2016YJCX76.

REFERENCES

1. Kaiser, J. A., "The Archimedean two-wire spiral antenna," *IRE Trans. Antennas Propag.*, Vol. 8, No. 3, 312–323, 1960.
2. Rahman, N., Q. Junhui, A. Sharma, V. A. Tran, M. N. Afsar, and R. Cheung, "Beam-width control using a cavity-backed elliptical Archimedean spiral antenna," *2011 IEEE Aerospace Conference*, 1–9, 2011.
3. Nakano, H., S. Sasaki, H. Oyanagi, and J. Yamauchi, "Cavity-backed Archimedean spiral antenna with strip absorber," *IET Microwaves, Antennas & Propagation*, Vol. 2, No. 7, 725–730, 2008.
4. Fang, H. R., M. Serhir, R. Balakrishnan, and R. Guinvarc'h, "Low profile cavity-backed four-arm Archimedean spiral antenna with 8 : 1 bandwidth," *The 8th EuCAP*, 2528–2531, 2014.
5. Mohamad, S., R. T. Cahill, and V. Fusco, "Selective high impedance surface active region loading of Archimedean spiral antenna," *IEEE Antennas and Wireless Propagation Letters*, Vol. 13, 810–813, 2014.
6. Schreider, L., X. Begaud, M. Soiron, B. Perpere, "Design of a broadband Archimedean spiral antenna above a thin modified Electromagnetic Band Gap substrate," *2006 FEC on Antennas and Propagation*, 1–4, 2006.
7. Ding, C. Y., C. L. Ruan, and L. Peng, "A novel Archimedean spiral antenna with uniplanar EBG substrate," *2008 ISAPE*, 313–315, 2008.
8. Shire, A. M. and F. C. Seman, "Parametric studies of Archimedean spiral antenna for UWB applications," *2014 IEEE APACE*, 275–278, 2014.
9. Tran, P. N. and S. K. Sharma, "An Archimedean spiral antenna loaded with superstrate and backed by 3D printed ground structure for directional patterns," *IEEE International Symposium on Antennas and Propagation*, 1829–1830, 2016.
10. Peng, L., J. Y. Xie, K. Sun, X. Jiang and S. M. Li. "Resonance based reflector and its application in uni-directional antenna with low-profile and broadband characteristics for wireless applications," *Sensors*, Vol. 16, No. 12, 2092, 2016.
11. CST Microwave Studio [Online], Available: http/www.cst.com.
12. Liu, Q., C. L. Ruan, L. Peng, and W. X. Wu, "A novel compact Archimedean spiral antenna with gap-loading," *Progress In Electromagnetics Research Letters*, Vol. 3, 169–177, 2008.
13. Peng, L., K. Sun, J. Y. Xie, Y. J. Qiu, and X. Jiang, "UWB bi-directional bow-tie antenna loaded by rings," *Journal of the Korean Physical Society*, Vol. 69, No. 1, 22–30, 2016.